ORIGINAL ARTICLE SPECIAL ISSUE: Intelligent and precision manufacturing with automation technology
Guest edited by Guo-Hua Feng

An Intelligent Fault Diagnosis System for Machine Tools

Chia Wang*, Wei-Yen Lin, and Hong-Tsu Young
Department of Mechanical Engineering, National Taiwan University, Taiwan
(**Received** 20 January 2014; **Accepted** 5 March 2014; **Published** on line 1 September 2014)
*Email: d00522025@ntu.edu.tw
DOI: 10.5875/ausmt.v4i3.525

Abstract: An automatic intelligent system is developed to diagnose shaft fault types. Features related to shaft faults are extracted from vibration signals to effectively identify the corresponding fault condition. Feature extraction is accomplished using Fourier Transform, empirical mode decomposition (EMD) and multi-scale entropy (MSE). Through the EMD method, the model uses characteristics of intrinsic mode functions (such as zero-crossing rate and energy, to represent shaft condition features. MSE is used to calculate the entropy of multi-scale of the signal. At a larger MSE scale, the MSE result can be used to clearly identify some shaft defect types. The conventional approach to monitoring of a machine's health online based on linear time-frequency analysis is subject to limitations, as the mechanical vibration signal is nonlinear and non-stationary in nature. Thus this research develops a diagnostic system based on the implementation of Fourier, EMD and MSE-based methods. In the buildup stage a knowledgeware is created from a database of existing defect types. Finally, the automatic intelligent monitoring system is implemented in a machine tool manufacturing company to verify its performance.

Keywords: EMD; IMF; Zero-Crossing Rate; MSE; Shaft; Diagnosis

Introduction

Increased global competition has prompted machine tool manufacturers to seek to reduce costs and time related to equipment repairs. Online condition-based automatic intelligent systems have been found to be an efficient strategy for achieving these ends [1].

Traditional diagnosis techniques used different aspects of linear technology, such as time, frequency, time-frequency analysis, or second (fourth-)-order statistics, to perform the fault vibration signals. But the vibration signals emitted by shafts with faults are nonlinear and non-stationary, and thus diagnostic performance is restricted by the limitations of linear analysis, making it very difficult to accurately evaluate the working condition of the shafts. Nonlinear techniques allow for the extraction of intrinsic patterns hidden within the dynamics of the system that may not be effectively identified using linear methodologies. Over the past decade a variety of nonlinear parameter methods have been introduced for machine fault diagnosis, such as the correlation dimension and Lempel-Ziv complexity. A brief review of their application for the analysis of mechanical vibration signals can be found in [2].

Another nonlinear approach is to measure the system complexity that quantifies the irregularity of a time series. Introduced by the authors in [3], multi-scale entropy (MSE), measures complexity by taking into account multiple time scales, computing sample entropy for each scale. The MSE measurement has been used to analyze the health of biological signals including ECG [4] and EEG signals [5, 6].

Biological signals and mechanical vibration signals are both nonlinear and non-stationary. Inspired by the success of applying MSE to monitor biological systems, researchers have recently applied MSE to monitor the health of machines. The authors in [2] applied A_E to monitor the condition of rolling bearings, while [7, 8] used MSE to analyze bearing-health conditions. In [9] MSE was used to monitor normal and misaligned shafts, and [10] used MSE to study the lifespan of machine tools.

Empirical Mode Decomposition (EMD) is an algorithm which uses the local characteristic time scale to decompose complex signals to a number of Intrinsic Mode Functions (IMFs) with physical meanings [11, 12]. By analyzing each IMF component, the characteristic information of the original signal could be extracted more accurately and effectively. An IMF represents a simple oscillatory mode compared with the simple harmonic function. In mechanical applications, one IMF would include one or more vibration mechanisms of similar waveforms and frequency ranges. Therefore, EMD is considered a self-adaptive signal processing method that can be applied to nonlinear and non-stationary processes. EMD has been incorporated to overcome the limitations of the Fourier transform [13, 14].

In addition to the traditional FFT method, this research presents an online feature extractor using MSE and EMD. Shafts with normal (i.e., qualified, healthy) and abnormal conditions (i.e., insufficient or excessive grease or pressure) are distinguished by observing the patterns of their MSE and EMD curves.

The measured vibration signal is filtered first. Then, their MSE and EMD curves are calculated and used as an index for feature identification. An adaptive algorithm is then used to compute MSE and EMD to achieve online computation.

System Architecture

Figure 2(a) shows the shafts with SKF R000645/205 bearings used as specimens to verify the proposed algorithm. The measurement system and parameters are introduced and discussed as follows.

Chia Wang is a PhD candidate at the Department of Mechanical Engineering at National Taiwan University. His research interests include artificial neural networks, vibration signal processing, software development, big data analysis and manufacturing management.

Wei-Yen Lin received his PhD in Mechanical Engineering from National Taiwan University. His research interests focus on vibration signal processing, software development, big data analysis and manufacturing management.

Hong-Tsu Young is Professor of Mechanical Engineering at National Taiwan University. His research interests focus on femtosecond laser processing, wafer ultra-precision grinding, CAM & the application of five-axis machining, and mechanical systems integration.

A PC-based instrument is developed in C and LabView to provide a flexible measurement system.NI-USB 9234 and cDAQ-9172 were chosen for data acquisition, and 352C65 ICP accelerometers (sensitivity, 100 mV/g) were used to collect vibration signals from the machine tools. As shown in Figure 2(a) the 352C65 ICP accelerometers were mounted magnetically on the front-side bearings of the shaft. The vibration signals are then acquired by the NI-USB 9234 and processed by the analysis software. NI LabView was used to develop the user interface (Figure 2(b)) which provides a real-time display of vibration signals from the accelerometers for analysis with the FFT, EMD, and MSE algorithms. The features of the calculated results are then applied to identify the shaft fault types, as shown in Figure 2(c). Finally, all the diagnosis results were recorded in the database. All confirmed data could then be compared to every unidentified shaft vibration signal for diagnosis.

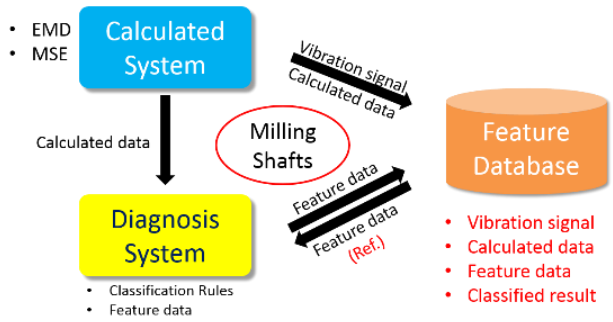

Figure 1. PC-based measurement full system chart includes sensor, user interface, calculation system, diagnosis system, and features database.

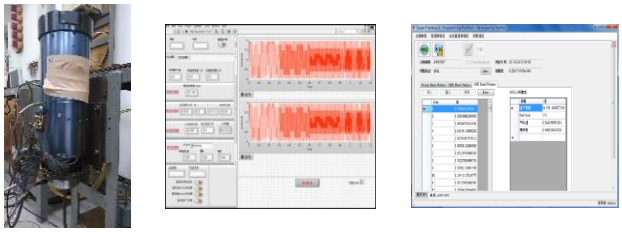

(a) (b) (c)

Figure 2. The experimental setup: (a) mounting setup, (b) LabView UI (calculation system) and (c) the program written in C language (diagnostic system).

Experiments Setup

All experiments were carried with the following parameters: signals were acquired at a maximum sampling rate of 51200 Hz; the maximum testing rotational speed was 24000 rpm, 400 Hz; the accelerometers were mounted magnetically on the front-side bearings of the shaft; and total measurement time was 5 sec. Figure 3 shows an instance of the measured vibration signals of one qualified shaft (number Q), while Figure 4 shows it's the corresponding

Fourier spectrum of the vibration signals. The figures indicate that the first-order frequency (1xRPM, 400 Hz) is the dominant constituent in the spectrum.

Experiments were run on both normal (qualified) and abnormal shafts. The abnormal shafts are listed in Table 1 with the following conditions: insufficient grease, excessive grease, insufficient preloading, excessive preloading, and bearing damage. All shafts were built by an experienced machining company. Prior to experimentation, the condition of all shafts was verified using reliable and well-accepted methods including dial gauges, thermocouple, FFT and RMS. "Excessive grease" and "insufficient grease" were defined according to standards provided by the machining firm. Defective bearing is defined as the surface of bearing being worn.

Figure 4 shows the Fourier spectrums of the vibration signal. The power distributions of the qualified shafts are dissimilar, thus the linear method based on frequency is not an appropriate approach to analyze vibration signals in this experiment.

The MSE curves are used to compare the relative complexity of the normalized time series (same variance for finest scale) based on the following guidelines:

(1) If, for the majority of the scales, the entropy values are higher for one time series than for another, the one with the higher entropy values is considered more complex;

(2) A monotonic decrease of the entropy values indicates the original signal contains information only in the smallest scale. Here, we adopt the MSE as a mathematical tool to quantify the machine health condition by quantifying the complexity of the machine system.

The EMD has been shown to decompose the time series into a number of IMFs which have some physical meanings [11, 12]. An IMF represents a simple oscillatory mode compared with the simple harmonic function. In mechanical applications, one IMF would include one or more vibration mechanisms which have similar waveforms and frequency ranges. After decomposing the signals into IMFs, the feature vectors could be computed with the zero-crossing rate and the average energy [13, 14].

Analysis Results

In this section, the MSE and EMD are used to analyze the specimens described in Table 1. The patterns of the MSE and EMD results are then used to distinguish shafts with different conditions.

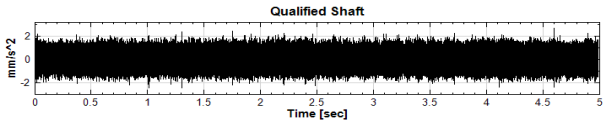

Figure 3. The vibration signal of the qualified shaft [Q1].

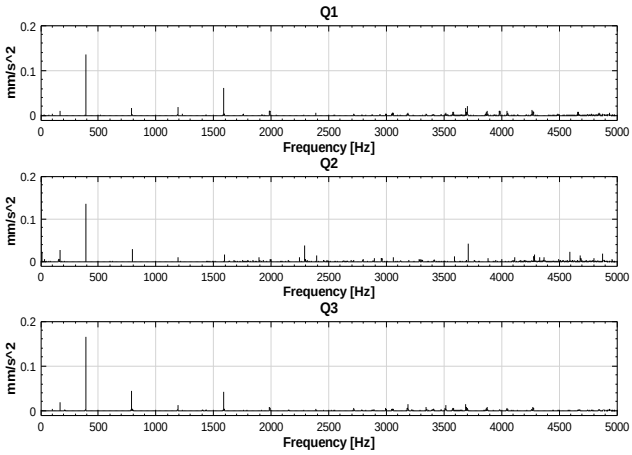

Figure 4. Fourier spectrum of the Q1 (top), Q2 (middle), and Q3 (bottom) shafts. (24000 rpm, 400 Hz)

Table 1. Different shaft conditions used in the experiment.

Condition	Number of Specimens
Qualified	5
Bearing defect	5
Insufficient grease	5
Excessive grease	5
Insufficient preloading	5
Excessive preloading	5

EMD diagnosis

After decomposing the signals into IMFs, the feature vectors could be computed with the zero-crossing rate and the energy. The calculated results for the Qualified Shaft are listed in Table 2.

Table 2. EMD diagnosis results for the Qualified Shaft.

IMF Number	Zero-Crossing Rate	Average Energy	Is target	Order	Percentage
IMF1	15020.5	0.009	No	-	-
IMF2	6694.4	0.009	No	-	-
IMF3	3535.6	0.004	Yes	9.3625	0.086
IMF4	1601.5	0.004	Yes	4.3098	0.057
IMF5	402.5	0.027	Yes	1.148	0.743
IMF6	217.5	0.003	Yes	0.5748	0.113
IMF7	119.8	0	No	-	-
IMF8	54.9	0.001	No	-	-
IMF9	24	0.001	No	-	-
IMF10	11.3	0.001	No	-	-
IMF11	5.3	0.001	No	-	-
IMF12	3	0.001	No	-	-
IMF13	1.3	0.003	No	-	-
IMF14	0.6	0.004	No	-	-
IMF15	0.1	0.001	No	-	-

As seen from Table 2, the zero-crossing rates of IMF1 and IMF2 are both over 5000 Hz. Obviously both IMF1 and IMF2 fall in the response-distortion range in

view of magnetically mounting. Other data show that the zero-crossing rates of IMF7 and above are less than 200 Hz which means half of the first order frequency is neglected. Therefore, only IMF3, IMF4, IMF5, IMF6 constitute the target IMFs while order equals zero-crossing rate divided by the working speed. The zero-crossing rate of IMF5 is 402.5, and its energy percentage is 74.3%, which indicates that the first order frequency component was decomposed into IMF5.

The data of all defect models were transformed to feature vectors and imported into the feature database. The EMD feature vectors of each fault condition are listed in Table 3. A rule of thumb shows that 3 feature vectors (4 target IMFs) will be extracted if the shaft is qualified, 4 feature vectors will be extracted when the shaft is defective, and 5 feature vectors will be extracted when the shaft is damaged.

Table 3. Feature vectors of all defect models.

Condition	Shaft Number	No. of Feature Vectors	Feature Vectors
Qualified	Q	3	(0.57,0.63)(3.16,-0.69) (5.05, 0.03)
Less-Preload	LP	4	(0.44,0.10)(1.08,0) (2.17,0.10)(3.54, 0.38)
Over-Preload	OP	4	(0.36,0.20)(0.92,0.1) (2.66,-0.2)(3.71, 0.30)
Less-Grease	LG	4	(0.34,0.09)(0.61,0.21) (1.87,-0.14)(3.12,0.17)
Over-Grease	OG	4	(0.37,0.03)(0.64,0.03) (1.29, 0.06)(2.96,0.69)
Bearing Defect	BD	5	(0.41,0.01)(0.76,0.03) (1.40,0.10)(2.61,0.21) (5.85, 0.03)

MSE diagnosis

Figure 5 shows the mean of the MSE curves for the six different qualified conditions Q, BD, LG, OG, LP, and OP running at different time windows. Starting from scale one, the entropy value increases quickly and then decreases to a certain value. It then begins to oscillate, and the amplitude of the oscillation decreases with scale, except for insufficiently greased shaft.

Based on the MSE curves and features, the classification rules were found to be able to identify six kinds of shaft status using three classification rules as follows:

Feature (1): Is $S_E(\tau=128) = 0$?

The entropy value is zero for the Q, LG, and OG conditions. It is potentially difficult to determine whether the entropy is zero due to statistical and numerical errors. An alternative is to measure the degree of symmetry at scale 128 as discussed in the previous section.

Feature (2): Number of local maximum points on the MSE curve.

The oscillatory behaviors can be measured by the number of local maximum points on the MSE curve. A 5^{th}-order median filter is applied to filter out possible local jigsaw patterns before counting the number.

Feature (3): $\int_{\tau 1}^{\tau 2} S_E(\tau)$ (area of the MSE curve between scales from τ_1 to τ_2)

As noted in [15], integrating the entropy values over a predefined range of scales is an index of complexity. Based on all the MSE curves in Figure 5, we adopt the area as an indicator of the shaft health condition. Table 4 lists some values of features (1), (2), and (3). Using these features as guides, we present an MSE feature extraction algorithm written in natural language in Figure 6.

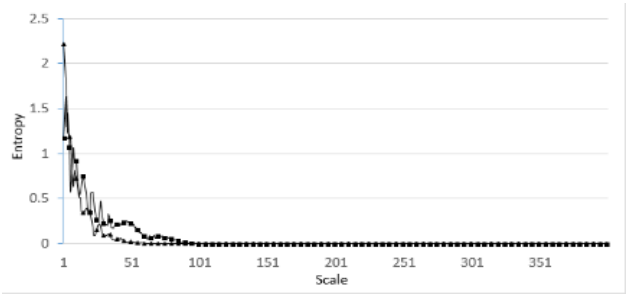

(a) ■ : Qualified; ▲ : Bearing Defect

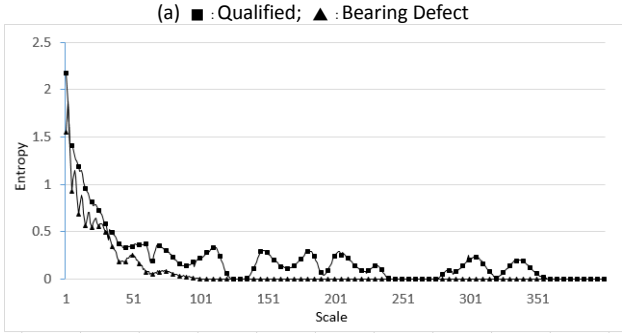

(b) ■ : Less Grease; ▲ : Over Grease

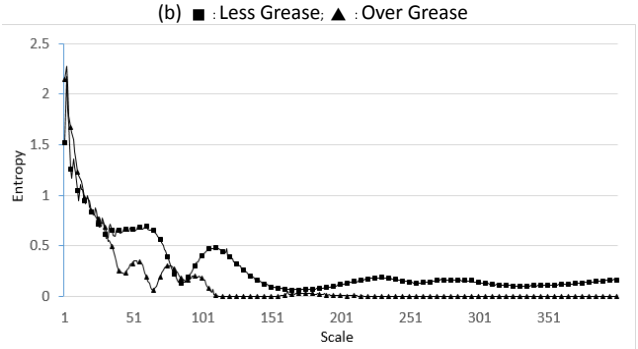

(c) ■ : Less Preload; ▲ : Over Preload

Figure 5. MSE profile (entropy versus scale) with m=2, r=0.15SD, scale=1:400 for N =10000, 7(a): Q and BD, 7(b): LG and OG, and 7(c): LP and OG.

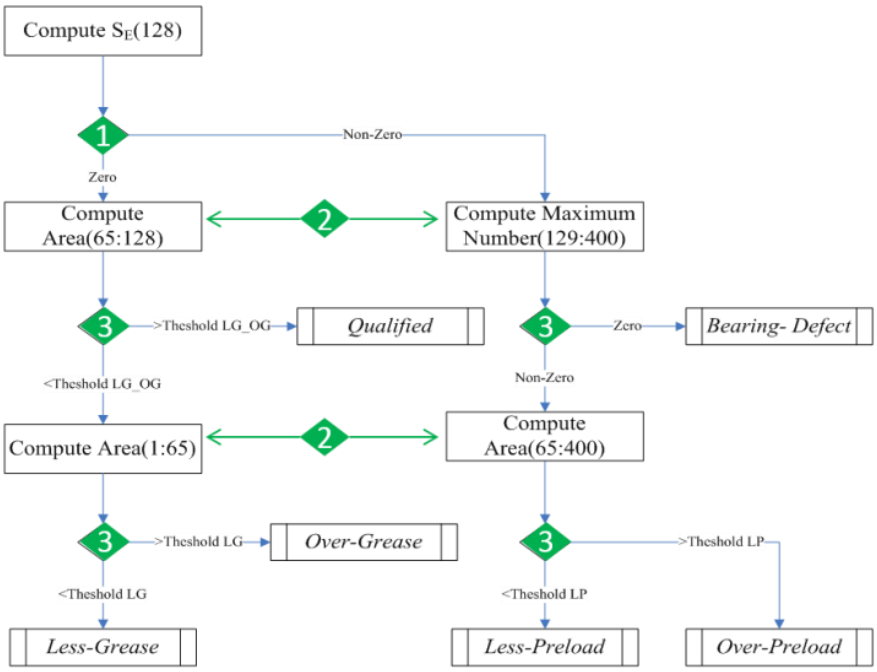

Figure 6. An MSE feature extraction algorithm written in natural language.

Summary

An automatic intelligent system is built including a user interface, calculation system, diagnostic system, and feature database (see Figure 7).

EMD and MSE are successfully used to analyze several common shaft defect modes. Experimental results show that:

(1) The number of the target IMFs reflects the condition of the shaft. The qualified shaft has four target IMFs, while shafts exhibiting faults including misalignment, insufficient grease, excessive grease, insufficient preloading and excessive preloading exhibit five target IMFs, and the shaft with the bearing defect has six.

(2) The pattern of feature vectors extracted from the IMF properties represents the condition of the shaft. Some defect models were added to a database to develop and train the knowledgeware.

(3) Conditions were successfully identified for the qualified shaft, along with those with insufficient grease and defective bearings. However, the models with insufficient preloading, excessive preloading and excessive grease could not be distinguished.

(4) Unlike the linear Fourier spectrum analysis, which shows different spectra for identical shaft health conditions, the MSE curve is uniform.

(5) The MSE curve shows different patterns for different health conditions, and the features of the different health conditions are clearly distinguished using the proposed feature extraction algorithm.

(6) An unknown shaft could be diagnosed with data from the knowledgeware using the correlation indicator of the proposed feature vectors.

Table 4: MSE curve features.

	Rule	Q	BD	LG	OG	LP	OP
1	$S_E(\tau=128) = 0$	True	False	True	True	False	False
	Area 1:64	49	49.	46.	57	59	75.
2	Area 65:128	11.2	0.34	5.7	0.9	2.4	11
	Area 65:400	21	6.2	11	9.5	12	33.
3	#max 129:400	4	0	1	2	1	2

After saving all the certified data, the automatic intelligent system can be used to clearly identify the shaft conditions. Reliability testing was conducted on a wide range of specimens with specific conditions and the diagnosis results are summarized in Table 5.

To compare the performance of the proposed online diagnosis system with others described in the literature, the Fourier spectrum, the empirical mode decomposition (EMD [11, 12, 16, 17]), and the single-scale entropy feature extractors are considered [11-13, 16, 17]. Both the Fourier spectrum and the EMD feature extractors measure the amplitude distribution in each mode (frequency) but the Fourier spectrum decomposes the signal into different sinusoidal harmonics, while the EMD decomposes the signal into different intrinsic modes.

The proposed system was used to analyze 423 shafts. In each test, the intelligent system was used first, with results then manually checked by experienced technicians.

The technicians followed a standard operating procedure established by their firm, methodically

checking each shaft using reliable and well-accepted methods, such as dial gauges, thermal couple, FFT and RMS. Comparing the analysis results of the proposed system and the technicians' manual assessment provides a statistical evaluation of the proposed system's accuracy and its average recognition rate. Table 5 summarizes the performance of the EMD, and MSE feature extractors. The identification of EMD for the qualified shaft and the bearing defect shaft have good recognition results, while shafts with another conditions have average identification rates of about 50%. Aside from the shaft with insufficient preloading, rates for shaft condition identification average above 60%.

Table 5 indicates whether or not the specimen was successfully identified. Fourier spectrum–based feature extractor can be used to identify the qualified shafts [13], but insufficient grease shafts are sometimes identified as qualified, while the others remain unidentified. The EMD-based feature extractor successfully identifies qualified, bearing-defect, and insufficient grease shafts, but not the others. The MSE feature extractor uses 3 features to successfully identify all conditions.

EMD and MSE are used to calculate the shaft vibration signals, and the classification rules of the two algorithms can be used to successfully identify several common shaft faults. This approach differs from previous methods in that it uses the temperature or RMS (Root Mean Square) to identify two kinds of result, under or over. The feature database provides data useful for identifying new classification rules. As the number of classification rules and algorithms increase, the identification rate can be expected to increase.

Future work will focus on incorporating additional specimen training data to help the system detect a wider range of defects.

Table 5. Matrix of diagnosis results with EMD-based and MSE-based feature extractors.

	EMD		MSE	
Models	Average recognition rate	Standard deviation	average recognition rate	Standard deviation
Qualified	87.77%	28.35%	60.70%	17.01%
Bearing Defect	100.00%	0.00%	69.96%	0.02%
Excessive Preloading	46.99%	7.31%	64.88%	5.36%
Insufficient Preloading	51.04%	9.79%	49.90%	18.55%
Insufficient Grease	44.39%	16.32%	65.82%	16.96%
Excessive Grease	54.88%	6.94%	71.16%	5.01%

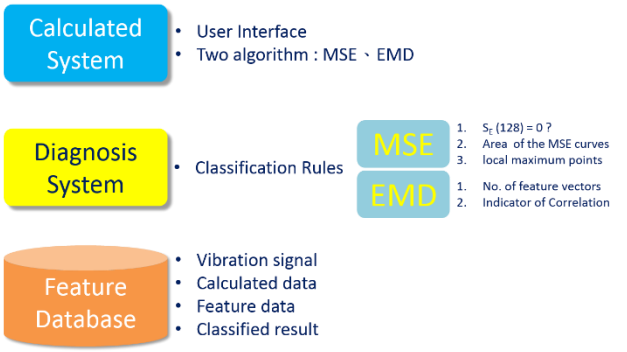

Figure 7. Full system structure, wherein the diagnosis system continuously improves through the addition of algorithms and classification rules.

References

[1] P. Tse, "Neural networks based robust machine fault diagnostic & life span predicting system," Ph. D. dissertation, The University of Sussex, United Kingdom, 1998.

[2] R. Yan and R. X. Gao, "Approximate entropy as a diagnostic tool for machine health monitoring," *Mechanical Systems and Signal Processing,* vol. 21, no. 2, pp. 824-839, 2007.
doi: 10.1016/j.ymssp.2006.02.009

[3] M. Costa, A. L. Goldberger, and C. K. Peng, "Multiscale entropy analysis of complex physiologic time series," *Physical Review Letters,* vol. 89, no. 6, pp. 068102, 2002.

[4] L. Angelini, R. Maestri, D. Marinazzo, L. Nitti, M. Pellicoro, G. D. Pinna, S. Stramaglia, and S. A. Tupputi, "Multiscale analysis of short term heart beat interval, arterial blood pressure, and instantaneous lung volume time series," *Artificial Intelligence in Medicine,* vol. 41, no. 3, pp. 237-250, 2007.
doi: 10.1016/j.artmed.2007.07.012

[5] X. Kang, X. Jia, R. G. Geocadin, N. V. Thakor, and A. Maybhate, "Multiscale entropy analysis of eeg for assessment of post-cardiac arrest neurological recovery under hypothermia in rats," *IEEE Transactions on Biomedical Engineering,* vol. 56, no. 4, pp. 1023-1031, 2009.
doi: 10.1109/tbme.2008.2011917

[6] S. F. Liang, H. C. Wang, and W. L. Chang, "Combination of eeg complexity and spectral analysis for epilepsy diagnosis and seizure detection," *EURASIP J. Adv. Signal Process,* vol. 2010, pp. 1-15, 2010.
doi: 10.1155/2010/853434

[7] L. Zhang, G. Xiong, H. Liu, H. Zou, and W. Guo, "An intelligent fault diagnosis method based on multiscale entropy and svms," in *Advances in neural networks – isnn 2009*. vol. 5553, W. Yu, H. He, and N. Zhang, Eds.: Springer Berlin Heidelberg, 2009, pp. 724-732.
doi: 10.1007/978-3-642-01513-7_79

[8] L. Zhang, G. Xiong, H. Liu, H. Zou, and W. Guo, "Applying improved multi-scale entropy and support vector machines for bearing health condition identification," *Proceedings of the Institution of Mechanical Engineers, Part C: Journal of Mechanical Engineering Science,* vol. 224, no. 6, pp. 1315-1325, 2010.
doi: 10.1243/09544062jmes1784

[9] J.-L. Lin, J. Y.-C. Liu, C.-W. Li, L.-F. Tsai, and H.-Y. Chung, "Motor shaft misalignment detection using multiscale entropy with wavelet denoising," *Expert Systems with Applications,* vol. 37, no. 10, pp. 7200-7204, 2010.
doi: 10.1016/j.eswa.2010.04.009

[10] Y. H. Pan, W. Y. Lin, Y. H. Wang, and K. T. Lee, "Computing multiscale entropy with orthogonal range search," *Journal of Marine Science and Technology,* vol. 19, no. 1, 2011.

[11] Z. S. Norden E. Huang, Steven R. Long, Manli C. Wu, Hsing H. Shih, Quanan Zheng, Nai-Chyuan Yen, Chi Chao Tung and Henry H. Liu, "The empirical mode decomposition and hilbert spectrum for nonlinear and non-stationary time series analysis," *Proceedings of the Royal Society A,* vol. 454, pp. 903-995, 1998.
doi: 10.1098/rspa.1998.0193

[12] N. E. Huang, Z. Shen, and S. R. Long, "A new view of nonlinear water waves: The hilbert spectrum," *Annual Reviews of Fluid Mechanics,* vol. 31, pp. 417-457, 1999.
doi: 10.1146/annurev.fluid.31.1.417

[13] W. Y. Lin and H. T. Young, "Development of manufacture execution system and fault diagnosis system," Ph. D. dissertation, Department of Mechanical Engineering, National Taiwan University, 2010.

[14] W. Y. Lin, L. C. Chuang, and H. T. Young, "Condition-based shaft fault diagnosis with the empirical mode decomposition method," *Proceedings of the Institution of Mechanical Engineers, Part B: Journal of Engineering Manufacture,* vol. 225, no. 5, pp. 723-734, 2011.
doi: 10.1177/2041297510394062

[15] H. G. Kang, M. D. Costa, A. A. Priplata, O. V. Starobinets, A. L. Goldberger, C. K. Peng, D. K. Kiely, L. A. Cupples, and L. A. Lipsitz, "Frailty and the degradation of complex balance dynamics during a dual-task protocol," *The journals of gerontology. Series A, Biological sciences and medical sciences,* vol. 64, no. 12, pp. 1304-1311, 2009.
doi: 10.1093/gerona/glp113

[16] N. E. Huang, M.-L. C. Wu, S. R. Long, S. S. P. Shen, W. Qu, P. Gloersen, and K. L. Fan, "A confidence limit for the empirical mode decomposition and hilbert spectral analysis," *Proceedings of the Royal Society of London. Series A: Mathematical, Physical and Engineering Sciences,* vol. 459, no. 2037, pp. 2317-2345, 2003.
doi: 10.1098/rspa.2003.1123

[17] N. E. HUANG and Z. WU, "Ensemble empirical mode decomposition: A noise-assisted data analysis method," *Advances in Adaptive Data Analysis,* vol. 01, no. 01, pp. 1-41, 2009.
doi: 10.1142/S1793536909000047